

Origami constraints on the initial-conditions arrangement of dark-matter caustics and streams

Mark C. Neyrinck¹

¹*Department of Physics and Astronomy, The Johns Hopkins University, Baltimore, MD 21218, USA*

20 July 2018

ABSTRACT

In a cold-dark-matter universe, cosmological structure formation proceeds in rough analogy to origami folding. Dark matter occupies a three-dimensional ‘sheet’ of free-fall observers, non-intersecting in six-dimensional velocity-position phase space. At early times, the sheet was flat like an origami sheet, i.e. velocities were essentially zero, but as time passes, the sheet folds up to form cosmic structure. The present paper further illustrates this analogy, and clarifies a Lagrangian definition of caustics and streams: caustics are two-dimensional surfaces in this initial sheet along which it folds, tessellating Lagrangian space into a set of three-dimensional regions, i.e. streams. The main scientific result of the paper is that streams may be colored by only two colors, with no two neighbouring streams (i.e. streams on either side of a caustic surface) colored the same. The two colors correspond to positive and negative parities of local Lagrangian volumes. This is a severe restriction on the connectivity and therefore arrangement of streams in Lagrangian space, since arbitrarily many colors can be necessary to color a general arrangement of three-dimensional regions. This stream two-colorability has consequences from graph theory, which we explain. Then, using N -body simulations, we test how these caustics correspond in Lagrangian space to the boundaries of haloes, filaments and walls. We also test how well outer caustics correspond to a Zel’dovich-approximation prediction.

Key words: large-scale structure of Universe – cosmology: theory

1 INTRODUCTION

On moderately large scales, matter and galaxies in the Universe trace what is known as a cosmic web (e.g., Bond et al. 1996). Regions well under the mean density develop into voids. At higher density, the matter is arranged into planar structures known as walls or pancakes. Still higher-density matter has a filamentary morphology. At the highest densities, it is assembled into pointlike clusters, or haloes.

There are several ways to characterize these structures. Observationally, one way of identifying and defining them is by looking for depressions, ridges, and peaks in the (over)density field δ . For example, one can measure the eigenvalues of the Hessian $\partial^2\delta/\partial x_i\partial x_j$; this gives local density maxima/ridges in one, two and three dimensions (e.g., Hahn et al. 2007; Aragón-Calvo et al. 2007; Sousbie et al. 2008; Pogosyan et al. 2009; Sousbie 2011). Another approach is global, defining voids to tessellate space. For instance, they can be defined as density depressions outlined by a watershed transform (Platen et al. 2007; Neyrinck 2008). In this framework, walls, filaments, and haloes are defined according to where voids meet each other, and the dimensionality of borders separating them (Aragón-Calvo et al. 2010). In

cosmology, these two definitions turn out to be rather similar, but this only is true in detail if no locally defined walls and filaments end within voids.

Another way to understand the structures is as folds in a three-dimensional manifold (‘sheet’), a Lagrangian picture. In Eulerian space, densities and velocities at fixed positions are tracked, but particles move around. But in Lagrangian space, each dark-matter parcel retains the same coordinates. First-order Lagrangian perturbation theory, known as the Zel’dovich (1970) approximation, already is quite useful to understand the basics of cosmological structure formation.

In this Lagrangian framework, particles in an N -body simulation can be thought of not simply as blobs of mass, but as vertices on an initially cubic grid that gravity deforms, and eventually causes to self-cross in three-dimensional position space. In six-dimensional velocity-position phase space, though, the manifold does not cross itself, a property which prompted our recent analogy to the paper-folding that occurs in origami (Falck et al. 2012). In that paper, we introduced a structure-finding algorithm (not to be confused with the origami analogy itself) called ORIGAMI (Order-ReversIng Gravity, Apprehended Mangling Indices) to identify structures in an N -body simulation according to the number of

axes along which the initial-conditions (Lagrangian) lattice has crossed itself. We briefly describe this algorithm below in the description of Fig. 3. A couple of other recent papers (Shandarin et al. 2011; Abel et al. 2011) have also explored the power of working within the dark-matter mesh. Shandarin et al. (2011) identify stream-crossings with overlapping tetrahedra from a tessellation of initial Lagrangian space. Abel et al. (2011) explore the benefits of measuring the density natively within the phase-space sheet, in principle greatly reducing particle-discreteness problems.

Another major application of a Lagrangian framework is the study of caustics, largely the subject of present work. A ‘caustic’ is the edge of a fold of the sheet in six-dimensional phase space. A strong observational motivation for studying caustics is that dark matter, if it annihilates, may do so most often in them, since formally the density goes arbitrarily high there. Thus they may greatly enhance observable signals from dark matter (e.g., Hogan 2001; Natarajan & Sikivie 2008; Vogelsberger & White 2011)

The behavior of caustics in Eulerian space has been extensively studied. Catastrophe theory allows a rigorous description and classification of the kinds of caustics and structures that can develop in Eulerian space when the manifold folds and crosses itself (e.g., Arnold et al. 1982; Arnold 2001).

A full understanding of the dynamics of the phase space sheet requires consideration of its symplectic structure, a special kind of geometry in which the position and velocity (sub)spaces do not directly mix on an equal footing. For example, the metric in a symplectic space considers the position and velocity spaces separately. In this paper, we do not explicitly consider the velocity subspace, concentrating on the spatial displacements between Lagrangian and Eulerian (both position) space. We note in passing, though, that the full dynamics of the sheet has special physical significance in general relativity, since the sheet consists of the set of observers that have experienced free-fall throughout cosmic time.

A Lagrangian view of the cosmic web, as we mainly adopt here, is difficult to apply directly to observed data; however, perhaps methods that construct initial conditions from observed data could in principle allow an avenue to do so (e.g. Mohayaee et al. 2006; Lavaux et al. 2008). And, for example, tracking caustics in simulations is relevant to the caustic method of estimating galaxy-cluster masses, which uses the outer caustics of cluster haloes as observed in red-shift space (Diaferio & Geller 1997).

This paper is organized as follows. In Section 2, we briefly review some properties of origami mathematics that are applicable in cosmology. In Section 3, we apply these properties to cosmology, giving Lagrangian definitions of the concepts of ‘caustics’ and ‘streams.’ We also explain some graph-theory consequences of the observation that streams are two-colorable according to their parity, and show some relevant measurements from N -body simulations.

2 ORIGAMI MATHEMATICS

Considering how ancient the art of origami is, the mathematics of it have developed relatively recently. A relatively early result (dating to 1893) is that paper-folding is a more pow-

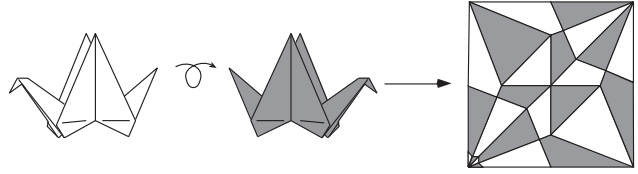


Figure 1. Two-coloring of the polygons outlined by creases in an origami ‘traditional Japanese flapping bird’ (similar to a crane). Polygons facing ‘up’ (out of the page in the leftmost diagram, with the head facing to the left) are colored white, while polygons facing ‘down’ (into the page in the leftmost diagram) are painted gray. The crane has been unfolded for the rightmost diagram. Creases are shown as lines here; the polygons outlined by them are successfully two-colored. Figure from Hull (2006), courtesy Tom Hull.

erful mechanism for solving geometric and algebraic problems than the classical ruler and compass. For example, in principle it can be used to trisect an angle, and to solve some types of cubic equations (Row 1966; Martin 1998; Hull 2006). Then, in the last few decades, significant advances were made in algorithmic origami design (e.g., Lang 2003).

Here we focus on some results in ‘flat origami’ that are particularly relevant to large-scale structure. In flat origami, folding of a two-dimensional sheet is allowed in three dimensions, but the result is restricted to lie flat in a plane, i.e. it could be squashed between pages in a book without acquiring any new creases. The class of flat-foldable origami is quite large, for example encompassing the famous paper crane, similar to the model shown in Fig. 1.

There are several theorems that have been proven about flat origami (e.g., Hull 1994, 2002). The main flat-origami result that we exploit in the present paper is the two-colorability of polygons outlined by origami crease lines. That is, two colors suffice to color them so that no adjacent polygons share the same color. Here ‘adjacent’ means sharing a crease line (not just a vertex).

To see why two colors suffice, consider the paper crane shown in Fig. 1. Both sides of it are shown, along with its appearance when unfolded. Each polygon is colored white or gray according to whether the polygon is facing ‘up,’ i.e. with the same orientation as it did initially, or ‘down,’ if it has been flipped over. This uniquely colors each polygon, and each crease does indeed divide ‘up’ from ‘down’ polygons.

A work of flat origami can be thought of as a function (a continuous piecewise isometry) mapping the unit square (the unfolded sheet at right in Fig. 1) into the plane. Each crease produces a reflection, reversing the direction of the vector on the paper perpendicular to the crease. The function is defined on each polygon by a sequence of these reflections. The color in each polygon corresponds to its parity, i.e. depending on whether the number of reflections used to define the function on that polygon is odd or even. It can also be measured locally with the determinant of the matrix defining the function on the polygon; we will also use this latter definition in the cosmological case below.

Besides two-colorability, there are other properties that flat-foldable crease patterns have. For example, Maekawa’s theorem states that in a flat-foldable crease pattern, the numbers of ‘mountain’ and ‘valley’ creases around a vertex (a junction of creases) differ by two. (A mountain crease

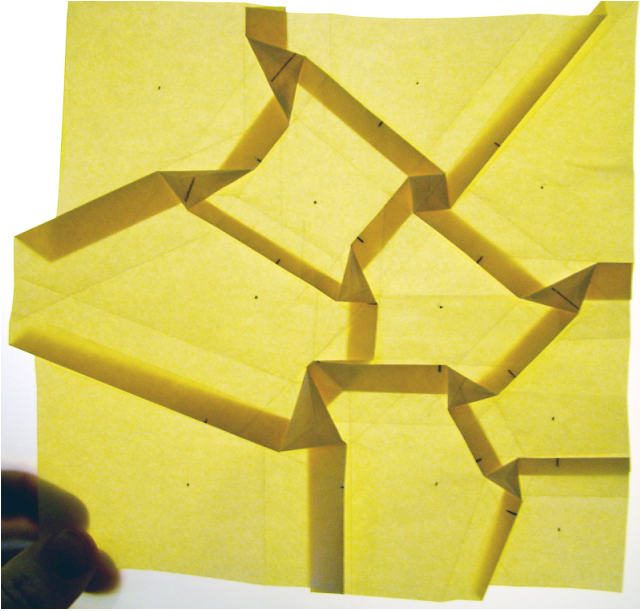


Figure 2. A Voronoi origami tessellation that bears some resemblance to cosmological voids, filaments and haloes. If the work were unfolded, the polygons outlined by creases would be two-colorable according to which way the polygon is facing. E.g. ‘voids’ and the topmost polygons in ‘haloes’ could be colored red, and the paper turned upside down within the ‘filaments’ could be colored green. The simple structure of ‘filaments’ and ‘haloes’ is as in the Zel’dovich approximation; the true universe has more complicated folding patterns, shown in subsequent figures. Figure by Eric Gjerde (<http://www.origamitessellations.com/>), used with permission.

becomes folded to form an upward-pointing ridge; a valley crease is folded in the opposite way.) In paper origami, two-colorability can be shown from Maekawa’s theorem (Hull 1994), so it may apply in some form to cosmological origami as well.

Even for paper origami, a difficult problem is to test that an arbitrary crease-pattern is physically flat-foldable without the paper intersecting any folds; this is an NP-complete problem (Bern & Hayes 1996). There are further results that, for instance, describe the angles around vertices, but they depend on the non-stretchability of the origami sheet, making them inapplicable to the cosmological case.

Fig. 2 shows a work of flat origami that bears some resemblance to a network of filaments and clusters in cosmology. Its ‘voids’ are Voronoi cells generated from the black points. Voronoi models of large-scale structure are good heuristic models of cosmological structure formation (e.g., Icke & van de Weygaert 1987; Kofman et al. 1990). The present figure corresponds most closely to a Zel’dovich-approximation evolution of particle displacements, in which structures fold up when expanding voids collide, but overshoot and do not undergo realistic further collapse. Many origami tessellations are described, with instructions, by Gjerde (2008).

3 APPLICATION TO COSMOLOGICAL STRUCTURES

Moving from paper origami to cosmological structure formation introduces a few changes. The manifold (sheet) has three instead of two dimensions. It folds in six dimensions (three position, and three velocity) instead of three. The sheet also stretches inhomogeneously in position space (all that we consider here), stretching more in voids than in dense regions. In phase space, on the other hand, there is no stretching if using a symplectic metric, since by Liouville’s theorem, symplectic volumes are conserved.

A consequence of the position-space stretchiness of the cosmological sheet is that, unlike in the paper-origami Fig. 2, creases need not extend indefinitely. For example, a pancake may form locally, without forming a full cosmic web.

With these caveats, folding of the three-dimensional sheet happens in an analogous way to as in the two-dimensional sheet of paper flat-origami. Caustics within the three-dimensional cosmological sheet are two-dimensional¹, just as caustics in two-dimensional origami paper are one-dimensional.

Importantly, the local parity on the sheet is easily defined, in the same way as in flat origami. At each position, define a first-order approximation of the mapping of mass elements (particles) from initial to final coordinates as a linear transformation (called the deformation tensor) plus a translation. If the spatial resolution in Lagrangian space (i.e. the mass resolution in a simulation) is sufficiently large compared to the scale on which Lagrangian space is folding, this linear transformation is meaningful. However, deep within a halo, the spatial relationships between Lagrangian neighbours in a practical N -body simulation may become essentially random, and this condition may not be satisfied.

We may use the determinant $J(\mathbf{q})$ of this deformation tensor to measure the parity (e.g., White & Vogelsberger 2009); as mentioned above, this definition can be used in two-dimensional flat origami, as well. For example, Vogelsberger & White (2011) use this parity measure to explore the rococo fine-scale structure of caustics in Eulerian space.

$J(\mathbf{q})$ gives the volume of a mass element that gets deformed by the tensor, times the parity. The elements of the deformation tensor are the components of initial-conditions Cartesian basis vectors transformed to the final conditions,

$$J(\mathbf{q}) = \det \left(\delta_{ij} + \frac{\partial \Psi_i}{\partial q_j} \right). \quad (1)$$

Here Ψ is the displacement field. For a mass element with Lagrangian position \mathbf{q} and Eulerian position \mathbf{x} , Ψ is defined by $\mathbf{x}(\mathbf{q}) = \mathbf{q} + \Psi(\mathbf{q})$. As usual in cosmology, we use comoving coordinates.

3.1 Streams and caustics in Lagrangian space

Caustics and streams are usually considered in Eulerian space. A caustic is a fold in projected phase space where

¹ As we discuss below, caustics that are lower-dimensional in Lagrangian space are in principle possible, but would require cylindrical or spherical collapse. In a realistic situation this never exactly happens; axes collapse one-at-a-time.

the density formally goes infinite if particle discreteness is ignored, and the density is smoothed on arbitrarily fine scales. As for streams, at a given Eulerian-space location \mathbf{x} , there may be many of them; each stream corresponds to a point in Lagrangian space that has ended up at \mathbf{x} .

In Lagrangian space, by analogy to an unfolded origami sheet, we define a stream as a contiguous three-dimensional region with the same parity. We define a caustic as a two-dimensional surface separating streams from each other. Defined this way, a caustic indeed corresponds to a fold, since the parity swaps if one moves across it.

By definition, space is tessellated by streams that are outlined by caustics. The streams are also two-colorable, since the parity may take only two values.

Two-colorability may seem hopelessly academic, and indeed it does not have obvious observational consequences. But in fact it greatly restricts the arrangement of streams in three-dimensional Lagrangian space. For a generic arrangement of solids in three or higher dimensions, the chromatic number (the number of colors required) is bounded only by the number of solids. To see this lack of bound, consider a stack of arbitrarily long raw spaghetti. Each may be slightly rotated from the last, in a way that it touches all others (Guthrie 1880). Now consider the connectivity of cooked spaghetti; it is easy to imagine a high chromatic number, without any special noodle-arrangement.

In summary, in two dimensions, origami-foldability reduces the maximum-possible chromatic number from 4 to 2. In the three-dimensional dark-matter sheet, foldability reduces the maximum-possible chromatic number of an arrangement of solids far more dramatically, from N_{streams} ($\sim 10^{14}$ at the Sun's location (Vogelsberger & White 2011)) to 2.

3.1.1 *Graph-theory properties of the stream tessellation*

In graph theory, a two-colorable graph is called bipartite (e.g., Chartrand & Zhang 2009). The vertices of our bipartite graph are the three-dimensional stream regions, and the edges (linking vertices together) are the caustic surfaces between them.

At least one whole book is devoted to the subject of bipartite graphs (Asratian et al. 1998); here we list a few of their properties, translating into cosmological terms. First, there is no path (stepping from stream to stream through caustics) starting and ending at the same stream that consists of an odd number of steps. Also, the adjacency matrix of streams has several properties that arise from bipartiteness.

Another result, König's Minimax Theorem, pertains to matchings in bipartite graphs. In our case, a 'matching' links pairs of streams such that each stream has a unique 'match' of the opposite parity. The theorem states that the maximum possible number of matches equals the 'minimum vertex cover,' the minimum number of streams needed to include in the graph such that all caustics touch at least one stream.

For example, imagine that only two isolated Zel'dovich pancakes form in a universe. In this case, there would be three Lagrangian streams: one positive-parity stream consisting of everything except the pancakes, and the two negative-parity collapsed patches. There are two caustics:

the boundaries between the negative-parity islands and the positive-parity sea around them. The maximum matching of positive to negative streams would have only one match: the initial-parity stream with either of the pancakes. By König's Minimax Theorem, this should equal the minimum vertex cover, and indeed it does: one stream (the positive-orientation sea) touches both caustics.

Considering the dual graph, in which streams and caustics swap roles, König has another result. His Coloring Theorem for bipartite graphs applies to the dual graph of caustics joined by streams: the chromatic number for the dual graph equals the maximum number of caustics around a single stream. If the graph of streams joined by caustics were not bipartite, the dual graph would generally have a larger chromatic number than the maximum number of caustics around a single stream.

3.1.2 *Discussion of the Lagrangian stream-caustic definition*

Before continuing on to measurements from simulations, we examine our definitions of streams and caustics a bit further, and problems that may arise from them.

A physical problem with our parity definition arises from a type of folding that is, in principle, possible in cosmology, but not in paper origami because the paper cannot stretch. Cosmological caustics may form in spherical or cylindrical collapse, not just planar collapse. Like planar collapse, spherical collapse reverses parity, but cylindrical collapse does not; it simply produces a 180° rotation in the two axes perpendicular to the cylinder.

However, in a physically realistic situation, the probability that more than one axis will collapse exactly simultaneously is zero. In the Zel'dovich approximation, for example, the deformation tensor will never have two exactly equal eigenvalues.

In a practical N -body simulation, the finite temporal and mass resolution will enable two- (and three-) axis crossings to happen between timesteps. In applying our parity definition to a simulation, we unfortunately miss some such unresolved caustics.

Another difficulty springs from numerical errors and errors (e.g. two-body effects) due to particle discreteness in a practical simulation. After many dynamical times suffering deep within a halo, Lagrangian mass elements may be hopelessly tangled for these reasons, and not just because of the doubtlessly plentiful caustics that have formed. Indeed, as shown in the figures below, halo regions have seemingly random parities, and it is not clear whether these parities arise from physical caustics, or this numerical 'noise.'

It may be difficult to visualize how a newly forming caustic forming in an already high-density region (already with many overlapping streams) behaves in Lagrangian space. In Lagrangian space, the caustic surface slices the various streams at various angles depending on how each stream has been rotated, stretched and reflected. But by definition, the new streams are still three-dimensional regions, divided by two-dimensional caustics.

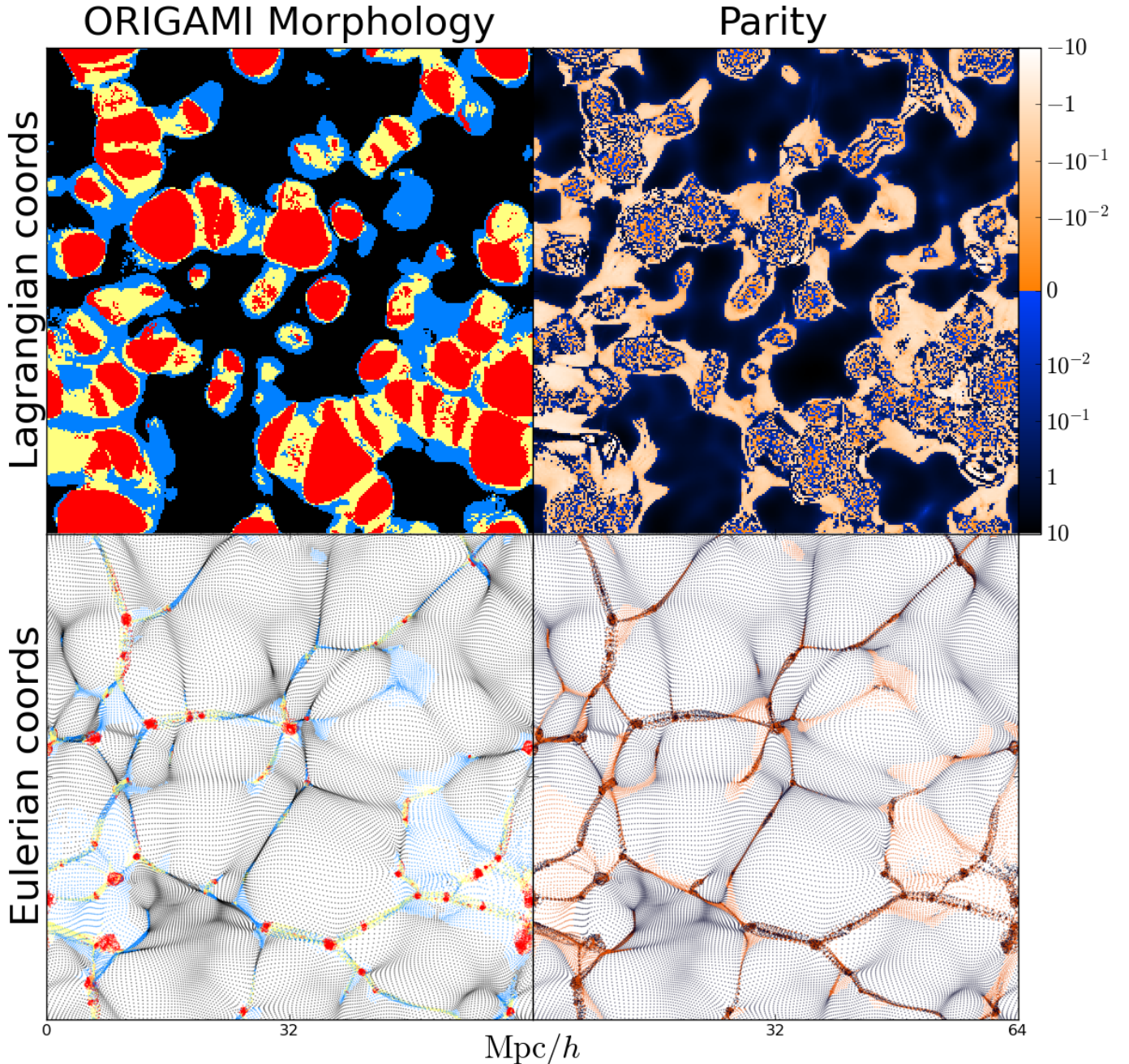


Figure 3. A 2D Lagrangian slice through a 3D Lagrangian cosmological sheet (top, unfolded; bottom, folded). Quantities were measured from a 256^2 sheet of particles from a 256^3 -particle Λ CDM N -body simulation; The 256^2 particles share the same z -coordinate in the initial-conditions lattice, where z points out of the page. Before running the simulation, the initial conditions were smoothed with a $1 h^{-1}$ Mpc Gaussian window, to inhibit small-scale structure formation. Top panels use Lagrangian coordinates, in which each particle is a square pixel in a 256^2 -pixel image. In the bottom panels, particles are shown in their actual present-epoch Eulerian (x, y) coordinates, projecting out the z coordinate (in which the slice does have some extent). At left, void, wall, filament and halo ORIGAMI morphologies are shown in black, blue, yellow and red, respectively. In right panels, particles are colored according to J , i.e. the volume of their fluid element times its parity. Black/blue particles have right-handed parity (as in the initial conditions), and white/orange particles have swapped, left-handed parity. The color scale was stretched around zero with the function $x \rightarrow \sinh^{-1}(10^3 x)$.

3.2 Simulation measurements

Fig. 3 shows the folding up of a two-dimensional Lagrangian slice of 256^2 particles from a three-dimensional 256^3 -particle gravitational simulation run to the present epoch. Pixels (in

Lagrangian coordinates) and particles (in Eulerian coordinates) are colored according to their ORIGAMI morphologies (left) and parities (right).

Panels at right show a measurement from an N -body simulation of the quantity we use to determine

the local parity, $J(\mathbf{q})$ from Eq. 1. This gives the volume of the mass element (inversely proportional to its density) times its parity. The parity can be read off from the color scale. Regions with right-handed parity (as in initial conditions) are black or blue; left-handed regions are white or orange. Each pixel represents a particle. In origami terms, this is the sheet before folding. Note that the magnitude is quite small in the cores of halo regions, because mass elements shrink considerably in high-density halo regions. To estimate the tensor at each particle, we use the final-conditions separations between the six particles that initially surround the particle, i.e. $\{\mathbf{x}_{i+1,j,k} - \mathbf{x}_{i-1,j,k}, \mathbf{x}_{i,j+1,k} - \mathbf{x}_{i,j-1,k}, \mathbf{x}_{i,j,k+1} - \mathbf{x}_{i,j,k-1}\}$, where the indices refer to positions on the Lagrangian particle grid. Note that the resolution of this measurement is twice the smallest available Lagrangian length scale (the interparticle spacing).

The morphology from the ORIGAMI algorithm (not to be confused with the origami-folding analogy itself) is shown in panels at left. A particle's ORIGAMI morphology depends on the positions of many other particles, not just (as in the parity measurement) its immediate Lagrangian neighbours. ORIGAMI measures morphologies by comparing particle orderings of along axes (rows and columns) in the initial Lagrangian lattice to their orderings in Eulerian space. Halo, filament, wall and void particles have been crossed (compared to the initial conditions) by some other particle along 3, 2, 1, and 0 orthogonal axes, respectively. That is, if we index particles in a row of the initial Lagrangian lattice, particles with Lagrangian indices i and j have crossed if $i < j$ but their order along that axis is swapped, i.e. their Eulerian positions $x_i > x_j$. Note that the total number of stream-crossings that a particle has undergone may be arbitrarily high, but the number of perpendicular axes along which these have happened is at most 3.

These ORIGAMI morphologies, and the parity colorings, correspond quite well to the locations of structures after folding. There are a few regions that would look voidy if they weren't colored, but are colored nonetheless (blue at left, and orange at right). These particles have crossed others in the direction perpendicular to the page.

The simulation shown was run to the present epoch using the GADGET-2 code (Springel 2005) with 256^3 particles in a box of size $64 h^{-1}$ Mpc, assuming a concordance Λ CDM set of cosmological parameters ($\Omega_b = 0.04$, $\Omega_m = 0.3$, $\Omega_\Lambda = 0.7$, $h = 0.73$, $n_s = 0.93$, $\sigma_8 = 0.81$). Before running the simulation, its initial-conditions density field was smoothed with a Gaussian of width $\sigma = 1 h^{-1}$ Mpc, inhibiting small-scale structure formation and clarifying the parity measurement. This smoothing reduced σ_8 (the dispersion in the overdensity within spheres of radius $8 h^{-1}$ Mpc) by 0.4 per cent. This small-scale power attenuation would happen in the real universe if the dark matter had substantial warmth; however, warm dark matter would also cause the three-dimensional 'sheet' it occupies to be smeared out by thermal motions.

There is some agreement between outer caustics identified by ORIGAMI morphology (the boundaries between black and non-black regions) and as defined by parity (the outermost boundaries between black/blue and white/orange regions), but the agreement is not perfect. There are a couple of reasons for this. First, the parity is defined on a larger grid spacing on the Lagrangian lattice (two interparticle

spacings, not one). Thus, if only one particle crossed another, this would be detected by the ORIGAMI criterion but not necessarily by the parity criterion. Second, the ORIGAMI algorithm detects crossings projecting along the Eulerian (x, y, z) axes; in contrast, the parity measurement uses only the local vectors between Lagrangian neighbours. So, unlike the parity measurement, the ORIGAMI morphology is in principle sensitive to large-scale rotations (fortunately, small on cosmological scales). Still, the ORIGAMI halo, filament and wall-finder shines here, where the smoothed initial conditions produce visually obvious morphologies.

Also note that streams need not have simple topologies. For example, the largest stream in Fig. 3 is just the 'void' stream, where no folding has occurred. This stream may in principle be entirely connected, and not split into isolated cells by caustics. Regions where folding has occurred may be isolated 'holes,' giving the void stream a non-trivial topology. Under our definition, curiously, a newly formed pancake has just one caustic associated with it: the entire surface separating the negative-parity region from the unfolded stream, even if kinematically it might seem more natural to define two caustics (the top and bottom of the pancake).

Fig. 4 is the same figure as Fig. 3, except that the simulation was run without smoothing the initial conditions. The small-scale structure in Fig. 4 makes the parity map (the upper-right panel) much more cluttered from additional structure. There are many visible extended streams (patches of identical parity), especially voids, but much of the plot looks essentially random. Halo particles (comprising most of the particles) have likely undergone many shell crossings. We again caution, however, that some of this apparent randomness could be from numerical 'noise.'

Fig. 5 shows Lagrangian $J(\mathbf{q})$ plots, adding red contours at the Zel'dovich-approximation (Zel'dovich 1970) prediction for the position of the outermost shell crossing. In the Zel'dovich approximation, the evolution with time τ of the volume V (in units of the mean) of a mass element at Lagrangian coordinate \mathbf{q} is given by

$$V(\mathbf{q}, \tau) = \prod_{i=0}^2 [1 - \lambda_i(\mathbf{q})D(\tau)], \quad (2)$$

a product over the three eigenvalues λ_i of the deformation tensor, using the linear growth factor $D(\tau)$.

For the Zel'dovich prediction in Fig. 5, we computed the largest eigenvalue of the deformation tensor (estimated as above) at each particle in the initial conditions at redshift $z = 75$. The red curve is the zero-contour of $[1 - \lambda_{\max}D(z = 0)]$, evolved forward to the present epoch with the ratio of growth factors $D(z = 0)/D(z = 75)$.

The agreement is rather good between the Zel'dovich prediction and actual outer-caustic locations for the smoothed simulation (left). For the unsmoothed simulation, the agreement is worse, but still not disastrous. It is not surprising that the Zel'dovich approximation works best at finding large-scale caustics.

4 CONCLUSION

In this paper, we further elucidate the analogy between structure formation in cosmology and origami. We illustrate an insight from origami mathematics that appears to

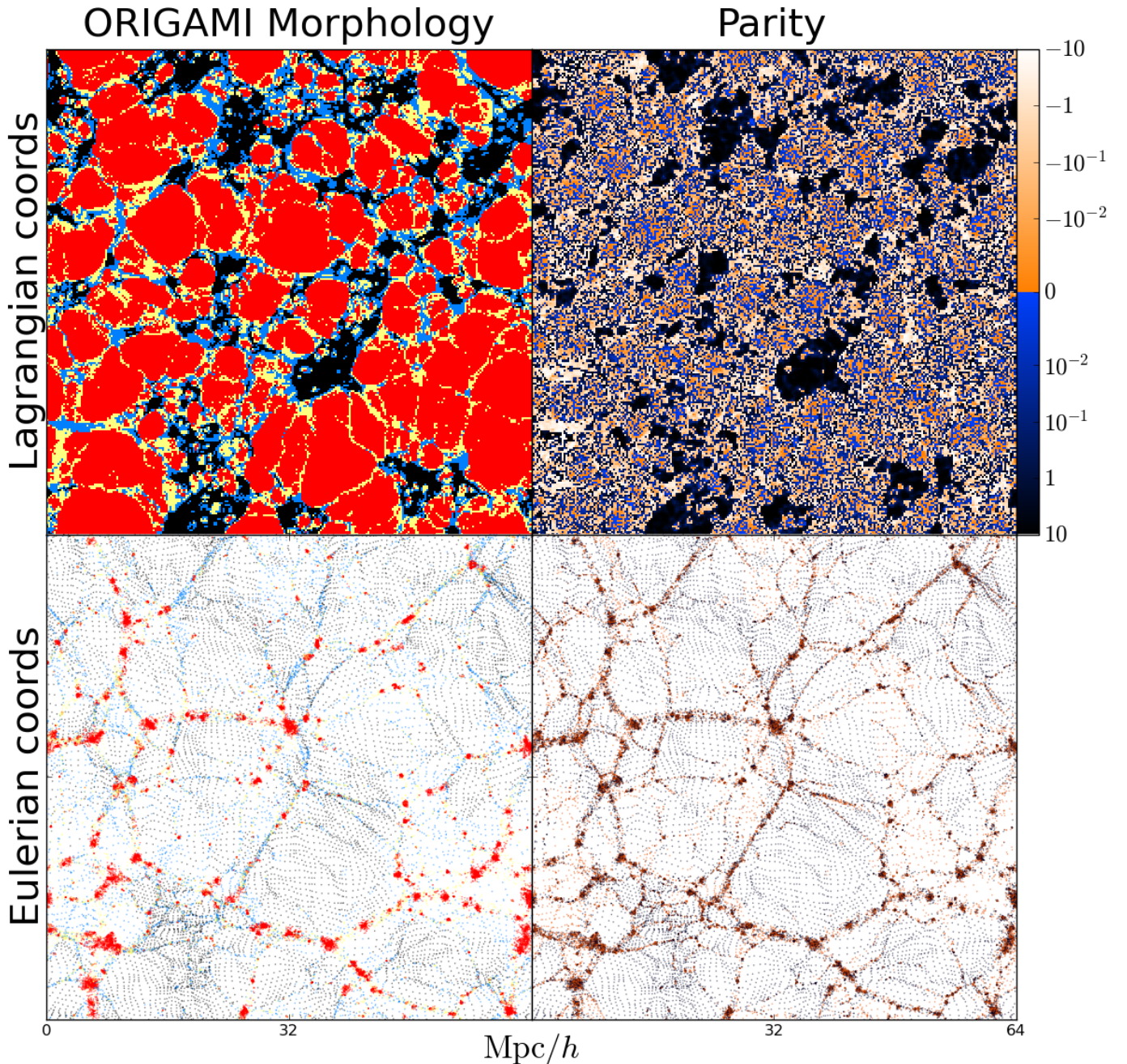


Figure 4. Same as Fig. 3, except measured from a simulation with full initial power, i.e. unsmoothed initial conditions.

be applicable to cosmology: the two-colorability of three-dimensional regions (streams) outlined by two-dimensional caustic surfaces in the initial conditions. That is, two colors suffice to color them such that adjacent regions do not have the same color, in the same way that four colors suffice to color any planar map. In fact, this result is rather trivial, if streams and caustics in Lagrangian space are defined as we do. However, a general arrangement of three-dimensional regions has no bound on the required number of colors, so this is a significant restriction on how dark matter can assemble itself into structures. Two-colorable graphs such as

this have many properties that may prove useful in understanding structure formation.

While much is known about the behavior and morphology of caustics and streams in Eulerian space, their behavior in Lagrangian space is also of interest. To our knowledge, this paper contains the first explicit illustration of the shapes of caustics and the streams in Lagrangian space. Many questions can be asked about them. What constraints exist on their topologies? Do Lagrangian caustics meet in one-dimensional curves (or zero-dimensional points), and what do these one- and zero-dimensional loci mean physically?

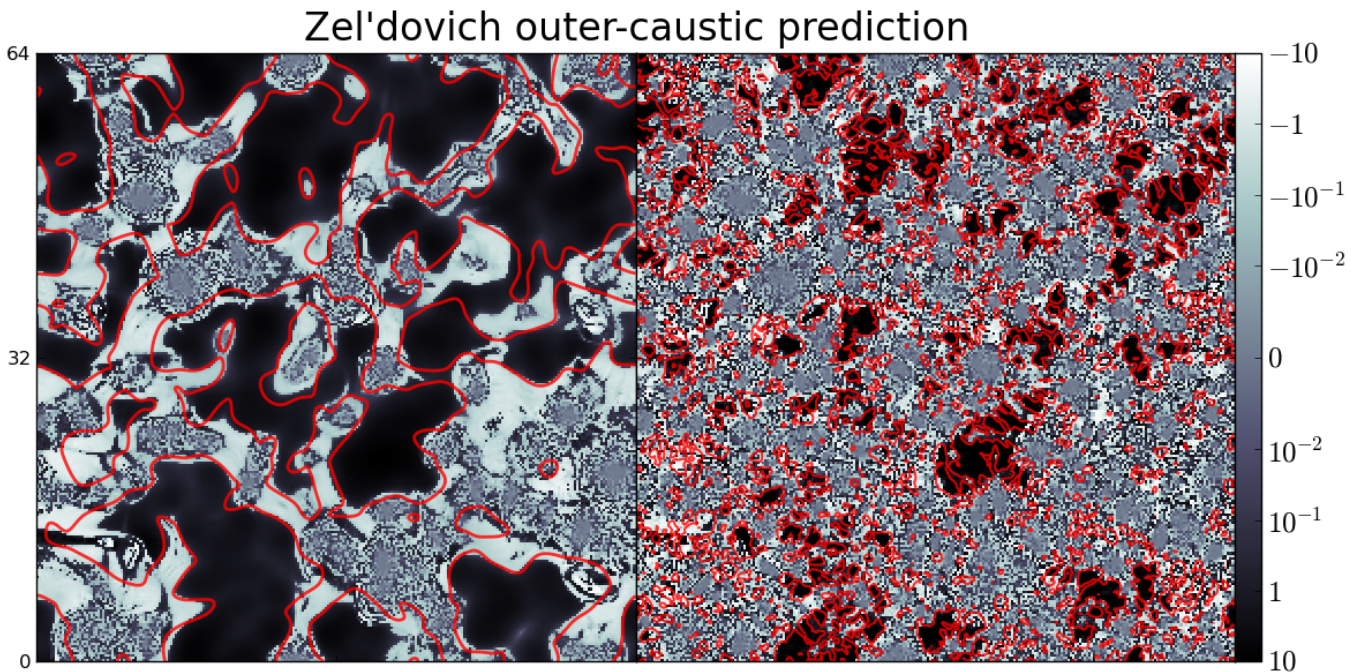


Figure 5. Comparison of a Zel'dovich prediction of where outer caustics should form (red contours) to where they actually do (boundaries between black and white regions), in the $64-h^{-1}$ Mpc simulations. In the left panel, the initial conditions have been smoothed, but not in the right panel. Pixels (corresponding to particles) are colored according to the present-epoch deformation tensor determinant $J(\mathbf{q})$. The plots under the red contours are same as the upper-right panels of Figs. 3 and 4, with a different color scale that hardly distinguishes small negative from small positive J . The red contours show the Zel'dovich prediction, i.e. the zero-crossing of the linearly extrapolated largest eigenvalue of the initial deformation tensor.

Admittedly, two-colorability in itself is lacking in obvious observational consequences, but it is closely tied to the process of caustic formation, of great interest for prospective dark-matter direct and indirect detection. As cosmological simulations push to smaller and smaller scales, departing farther and farther from comfortable linear-regime physics, it is useful to know as much mathematically as possible (including the present result) about the structures that develop. It would be interesting to explore whether enforcing the properties of caustics and streams found here, or of the three-dimensional sheet structure itself, would be useful to ‘clean’ numerical noise away from simulations.

The origami analogy also has substantial pedagogical, public-outreach value. Crease-patterns of a popular hands-on ‘fold your own galaxy’ activity, similar to Fig. 2, can be found at <http://skysrv.pha.jhu.edu/~neyrinck/origalaxies.html>.

ACKNOWLEDGMENTS

I thank Miguel Aragón-Calvo for the use of the simulations presented here, and for many discussions; Robert Lang for an inspiring colloquium about paper origami, and valuable discussions; Tom Hull for permission to use Fig. 1; Eric Gjerde for permission to use Fig. 2; Alex Szalay and Bridget Falck for fruitful discussions; and Tom Bethell for many useless discussions. I also thank the referee for insightful suggestions. I am grateful for support through Alex Szalay from the Gordon and Betty Moore Foundation.

REFERENCES

- Abel T., Hahn O., Kaehler R., 2011, MNRAS, submitted
Aragón-Calvo M. A., Jones B. J. T., van de Weygaert R., van der Hulst J. M., 2007, A&A, 474, 315
Aragón-Calvo M. A., Platen E., van de Weygaert R., Szalay A. S., 2010, ApJ, 723, 364
Arnold V., 2001, Singularities of Caustics and Wave Fronts, Mathematics and Its Applications. Springer
Arnold V. I., Shandarin S. F., Zeldovich I. B., 1982, Geophysical and Astrophysical Fluid Dynamics, 20, 111
Asratian A., Denley T., Häggkvist R., 1998, Bipartite graphs and their applications, Cambridge tracts in mathematics. Cambridge University Press
Bern M., Hayes B., 1996, in In Proceedings of the 7th Annual ACM-SIAM Symposium on Discrete Algorithms, pp. 175–183
Bond J. R., Kofman L., Pogosyan D., 1996, Nature, 380, 603
Chartrand G., Zhang P., 2009, Chromatic graph theory, Discrete mathematics and its applications. Chapman & Hall/CRC
Diaferio A., Geller M. J., 1997, ApJ, 481, 633
Falck B. L., Neyrinck M. C., Szalay A. S., 2012, ApJ, submitted
Gjerde E., 2008, Origami tessellations: awe-inspiring geometric designs, Ak Peters Series. A K Peters
Guthrie F., 1880, Proc. Roy. Soc. Edinburgh, 10, 727
Hahn O., Porciani C., Carollo C. M., Dekel A., 2007, MNRAS, 375, 489

- Hogan C. J., 2001, *Phys. Rev. D*, 64, 063515
- Hull T., 2006, *Project origami: activities for exploring mathematics*, Ak Peters Series. A.K. Peters
- Hull T. C., 1994, *Congressus Numerantium*, 100, 215
- Hull T. C., 2002, in *The Proceedings of the Third International Meeting of Origami Science, Mathematics, and Education*, T. C. Hull, ed., p. 29
- Icke V., van de Weygaert R., 1987, *A&A*, 184, 16
- Kofman L., Pogosian D., Shandarin S., 1990, *MNRAS*, 242, 200
- Lang R. J., 2003, *Origami design secrets: mathematical methods for an ancient art*, Ak Peters Series. A.K. Peters
- Lavaux G., Mohayaee R., Colombi S., Tully R. B., Bernardeau F., Silk J., 2008, *MNRAS*, 383, 1292
- Martin G. E., 1998, *Geometric Constructions*. Springer
- Mohayaee R., Mathis H., Colombi S., Silk J., 2006, *MNRAS*, 365, 939
- Natarajan A., Sikivie P., 2008, *Phys. Rev. D*, 77, 043531
- Neyrinck M. C., 2008, *MNRAS*, 386, 2101
- Platen E., van de Weygaert R., Jones B. J. T., 2007, *MNRAS*, 380, 551
- Pogosyan D., Pichon C., Gay C., Prunet S., Cardoso J. F., Sousbie T., Colombi S., 2009, *MNRAS*, 396, 635
- Row T. S., 1966, *Geometric Exercises in Paper Folding*. Dover
- Shandarin S., Habib S., Heitmann K., 2011, *ArXiv e-prints*
- Sousbie T., 2011, *MNRAS*, 414, 350
- Sousbie T., Pichon C., Colombi S., Novikov D., Pogosyan D., 2008, *MNRAS*, 383, 1655
- Springel V., 2005, *MNRAS*, 364, 1105
- Vogelsberger M., White S. D. M., 2011, *MNRAS*, 413, 1419
- White S. D. M., Vogelsberger M., 2009, *MNRAS*, 392, 281
- Zel'dovich Y. B., 1970, *A&A*, 5, 84